

# Dynamically Programmable Digital Tissue Phantoms

Steven W. Brown<sup>1</sup>, Joseph P. Rice<sup>1</sup>, David W. Allen<sup>1</sup>, Karel Zuzak<sup>2</sup>, Edward Livingston<sup>3</sup> and Maritoni Litorja<sup>1\*</sup>

<sup>1</sup>National Institute of Standards and Technology, Gaithersburg, MD, USA 20899

<sup>2</sup>University of Texas at Arlington, Arlington, TX 76109

<sup>3</sup>University of Texas Southwestern Medical Center, Dallas, TX 75390

## ABSTRACT

As optical imaging modalities gain acceptance for medical diagnostics and become common in clinical applications, standardized protocols to quantitatively assess optical sensor performance are required to ensure commonality in measurements and to validate system performance. The current emphasis is on the development of 3-dimensional, tissue-simulating artifacts with optical scattering and absorption properties designed to closely mimic biological systems. These artifacts, commonly known as tissue phantoms, can be fairly complex and are tailored for each specific application. In this work, we describe a conceptually simpler, 2-dimensional digital analog to the 3-dimensional tissue phantoms that we call Digital Tissue Phantoms. The Digital Tissue Phantoms are complex, realistic, calibrated, optical projections of medically relevant images with known spectral and spatial content. By generating a defined set of Digital Tissue Phantoms, the radiometric performance of the optical imaging sensor can be quantified, based on the accuracy of measurements of the projected images. The system is dynamically programmable, which means that the same system can be used with different sets of Digital Tissue Phantoms for sensor performance metrics covering a wide range of optical medical diagnostics, from cancer and tumor detection to burn quantification.

Keywords: Calibration, characterization, hyperspectral, medical imaging, spectroscopy, tissue phantom

## 1. INTRODUCTION

Optical system evaluation is a generic problem. Typical calibrated radiance or reflectance standards used by a calibration facility are designed to vary slowly spectrally and to be spatially uniform. They therefore do not approximate the optical medical scenes being measured by optical imagers and are inadequate to validate the performance of optical medical imaging systems. Consequently, biomedical imaging systems are evaluated and compared using reference tissue-simulating artifacts called phantoms, which are 3-dimensional structures designed to mimic the optical characteristics (absorption and scattering properties) of living tissue. In a review of tissue phantoms for optical use, Pogue and Patterson identified four categories for the use of tissue phantoms.<sup>1</sup> The first of these is for the validation of physical models and simulations. The other three summarily involve calibration and system validation. Optical tissue phantoms need to be reliably stable to support quantitative measurements by the optical instruments. However, the requirement to mimic tissue chemistry has led to the use of soft materials such as agar or gelatin, which allows compositional modifications using biologically relevant substances. This is a challenge since these soft materials have short shelf life and repeatability and reproducibility can be low. Availability of materials over a long period of time is also questionable.

As the applications for optical medical imaging systems have increased, so have the number and complexity of tissue phantoms. Phantoms are currently developed in an *ad hoc*, individual basis independent of any national standards organization recommendation. Consequently, no means currently exists to independently validate the efficacy of these phantoms for the calibration of optical medical imaging systems. This lack of standardization of optical phantoms means there are no common accepted methods for system evaluation and comparisons. Spectrophotometric data of biologically relevant substances are typically reported as relative data and have no units. In some cases, absorptivity values of substances are reported. In general, radiometric quantities are not measured which makes proper instrument validation and comparison difficult to accomplish.

In this work, we discuss a fully integrated radiometric characterization and calibration platform called a Hyperspectral

\*Correspondence: maritoni.litorja@nist.gov

Image Projector (HIP) that would have the capability of generating standardized sets of Digital Tissue Phantoms. Digital Tissue Phantoms are spatially complex scenes with user-defined, programmable spectra projected in each pixel in the scene.<sup>2,3,4</sup> Conceptually, as shown in Fig. 1, the HIP is a source analog to a hyperspectral imaging system, projecting a data hypercube.

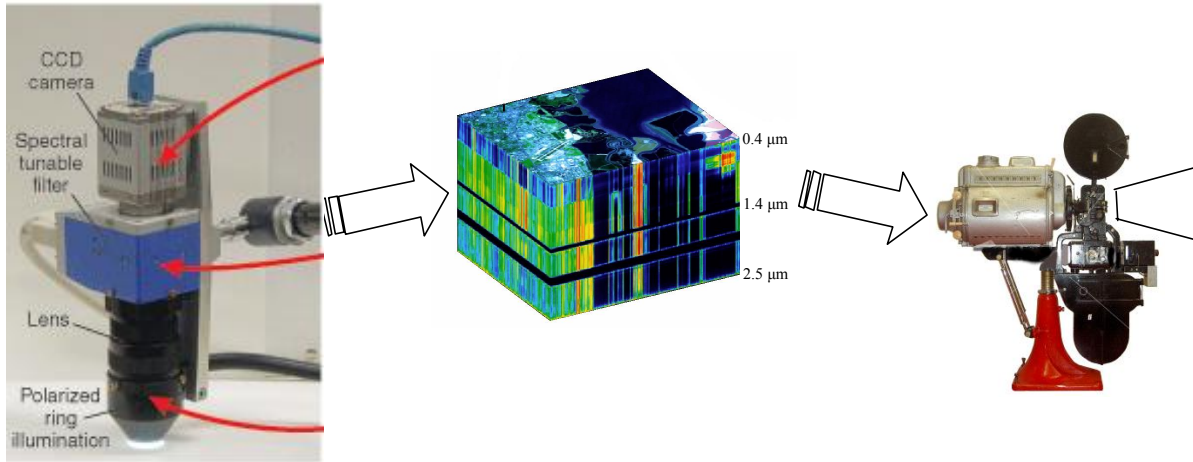


Figure 1. A hyperspectral imaging system, shown on the left, acquires a data hypercube, shown in the middle, where there is a unique spectral distribution associated with each pixel in the image. The Hyperspectral Image Projector, shown on the right, projects the data hypercube, projecting a unique spectral distribution in each pixel in the image.

The projected spectroscopic image, or Digital Tissue Phantom, can be a simulated one, based on a typical range of values for a type of tissue, or a specific hyperspectral data cube acquired by a reference hyperspectral imager. Ideally, the hyperspectral images would be traceable to the International System of Units (SI) and maintained in a reference library database. The HIP would provide a common, accepted platform to validate the performance of hyperspectral optical imaging systems. To validate an instrument's performance, a series of projected images would be measured by a calibrated reference instrument and the instrument under test. The projected images for a particular application would be defined by a medical standards organization. Values measured by the instrument under test would be compared to the values measured by the test instrument, and defined metrics would be used to assess the performance of the instrument under test.

This has the advantage of flexibility in scene composition—perturbations to the mean spectra can be injected to test for various elements in the optical system under test such as spatial resolution or sensitivity to spectral composition changes. This allows for system-level evaluation of both the imaging system and the data retrieval algorithm. The HIP is dynamically programmable and movies of projected scenes with changing spectral content can be projected. Finally, the system is flexible, and the same setup can project different libraries of images, so a common calibration facility can validate the performance of instruments that are used in a wide variety of applications.

The validation is based on measurements by the reference imager. The reference instrument would be sent to a primary calibration facility on a routine basis for calibration. The calibration is tied to primary national radiometric standards, and measurements by the reference instrument are traceable to the SI, with well-defined uncertainties. The instrument would be characterized for spatial and spectral scattered light, using protocols recently developed at the National Institute of Standards and Technology.<sup>5</sup> Based on these measurements, algorithms designed to correct the instrument's response for spectral and spatially scattered light will be developed and applied to the instrument's response function.

In Section 2, we describe the components of the HIP system, a Spectrally Tunable Source (STS) known as a Spectral Light Engine, capable of generating complex spectral distributions, and a Spatial Light Engine, capable of projecting the hyperspectral data cube. In Section 3, we describe the realized bench-top HIP system.

## 2. HYPERSPECTRAL IMAGE PROJECTOR (HIP)

The core of a HIP is Texas Instrument's Digital Micromirror Device (DMD).<sup>6</sup> The DMD is a two-dimensional array of individually programmable, aluminum micromirrors; one common DMD is a 1024 by 768 element array of 13.68  $\mu\text{m}$  square mirrors. Each mirror can be individually addressed to rotate about a diagonal axis. The rotation angles are fixed using hard post stops and range from 10° to 12°; in Fig. 2, a +10° rotation corresponds to the mirror 'on' state and -10° rotation corresponds to the mirror 'off' state.

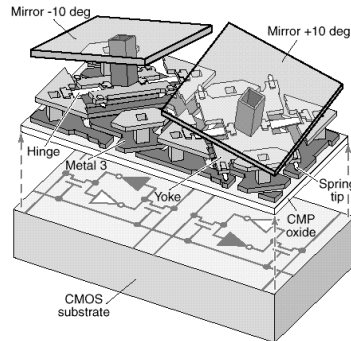


Fig. 2. Two micromirror elements in a DMD. Ref. 6.

The HIP system is conceptually similar to commercial Digital Light Processing (DLP) projection systems. In a DLP, shown schematically in Fig. 3,<sup>6</sup> light is focused through a rotating multi-color (typically red, green, and blue) filter wheel. The light then homogeneously illuminates a DMD-mirror array. Light from the DMD mirror array is projected onto a screen or other suitable medium using a projection lens. By varying the time that individual DMD mirrors are turned on within the period of time the light is incident on one of the primary colors making up the filter wheel, a different grayscale image of each color is projected onto the screen. The individual color grayscale images are combined (at the filter wheel rotation rate) to create a full rgb color image. In typical projection systems, scenes are updated at a rate of 50 Hz to 60 Hz.

The HIP system functions in the same basic fashion, except that both the number of input spectral distributions and their spectral content are user-defined. That is, the lamp and color filter wheel are replaced by user-defined input spectral distributions, created by the Spectral Light Engine. In addition, instead of 3 fixed spectral distributions, the number of spectral distributions input into the scene projector in a period is user-defined. In the simplest example, shown in Fig. 4, the basis spectra are represented by Gaussian distributions. The number of basis spectra increases from 3 in the filter-wheel projector to 20 in the HIP, covering the spectral range from 400 nm to 750 nm. A DLP projection system with the 3 basis spectra is able to reproduce the color in a particular image extremely well. With the 20 basis spectra, the HIP is able to significantly better reproduce the full spectral content in an image.

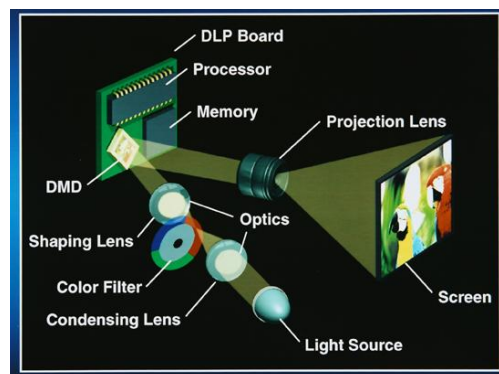


Fig. 3. Single chip DLP projection system layout. Ref. 6

Because the Spatial Light Engine uses time-division multiplexing to project the images, reducing the number of basis (or endmember) spectra increases the time, or maximum intensity, available for each spectrum. The remote sensing community has a great deal of experience de-convolving hyperspectral image data cubes into endmember (or basis) spectra. We used one such algorithm, the Sequential Maximum Angle Convex Cone (SMACC) algorithm,<sup>7</sup> to deconvolve an example remote sensing hyperspectral image into 7 broadband endmember spectra.<sup>3</sup> Figs. 5-7 demonstrate an example deconvolution of one medically-relevant hyperspectral data cube (Fig. 5) into 5 endmember spectra (Fig. 6) and abundance images Fig. 7. The abundance images are grayscale images representing the relative distribution of each of the 5 endmember spectra in the hyperspectral image.

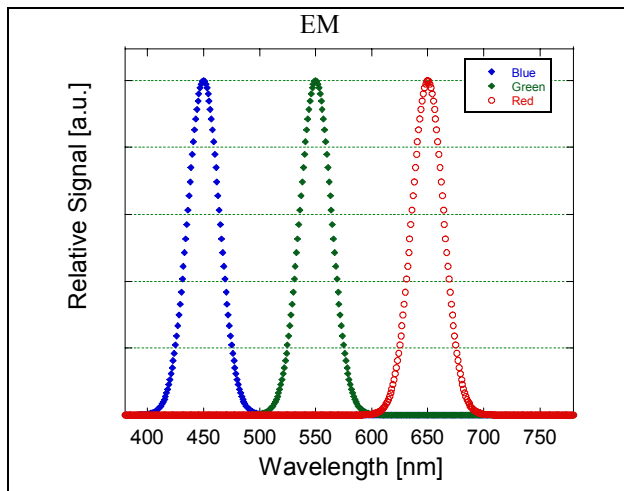


Fig. 4a. DLP red, green, and blue basis functions.

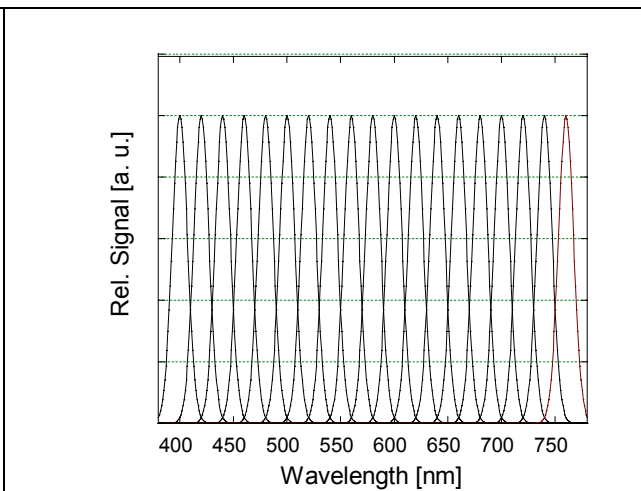


Fig. 4b. Example basis functions from a HIP.

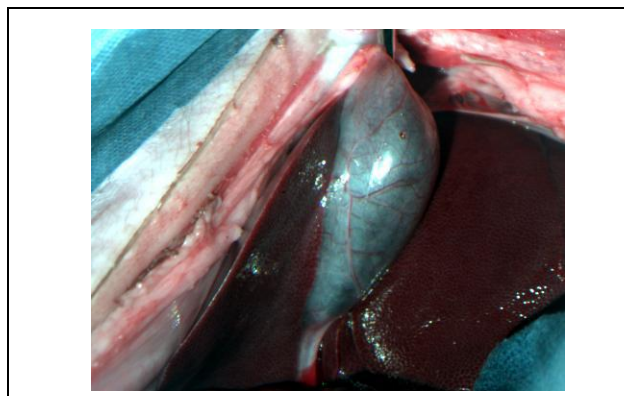


Fig. 5. Rgb image of a hyperspectral data cube of a gall bladder, liver, and skin image.

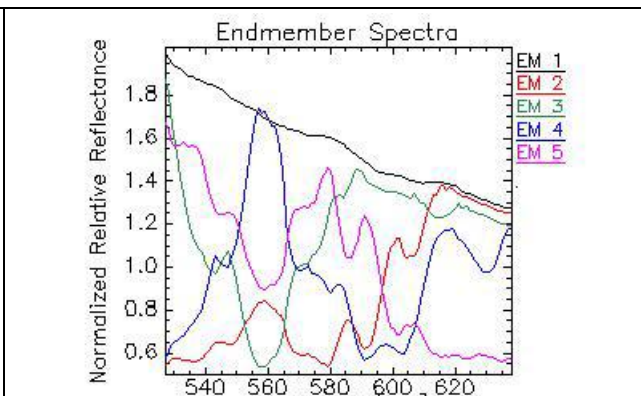


Fig. 6 Spectral distributions of 5 endmember spectra using the SMACC image deconvolution algorithm.

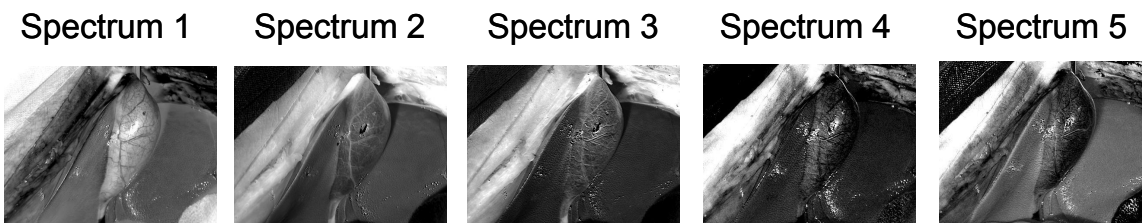


Fig. 7. Grey-scale abundance images for the 5 endmember spectral distributions shown in Fig. 6.

The user-defined HIP basis spectra are generated by a Spectral Light Engine.<sup>8,9</sup> Fundamentally, a spectral light engine is a spectrograph, with a DMD replacing the CCD at the focal plane of the instrument. Light reflected from DMD mirrors in the ‘on’ state is collected, homogenized, and directed onto the DMD in the Spatial Light Engine. Instead of synchronizing the DLP projector to a rotating filter wheel, in the HIP, the two DMD mirror arrays are synchronized. The HIP, consisting of a spectral engine coupled to a spatial engine, is schematically illustrated in Fig. 4. The spatial engine projects the basis spectra, in the correct proportions in each spatial region, sequentially to create a time-averaged spatially complex scene with realistic spectral content. In the following, the Spectral Light Engine and the Spatial Light Engine are described individually.

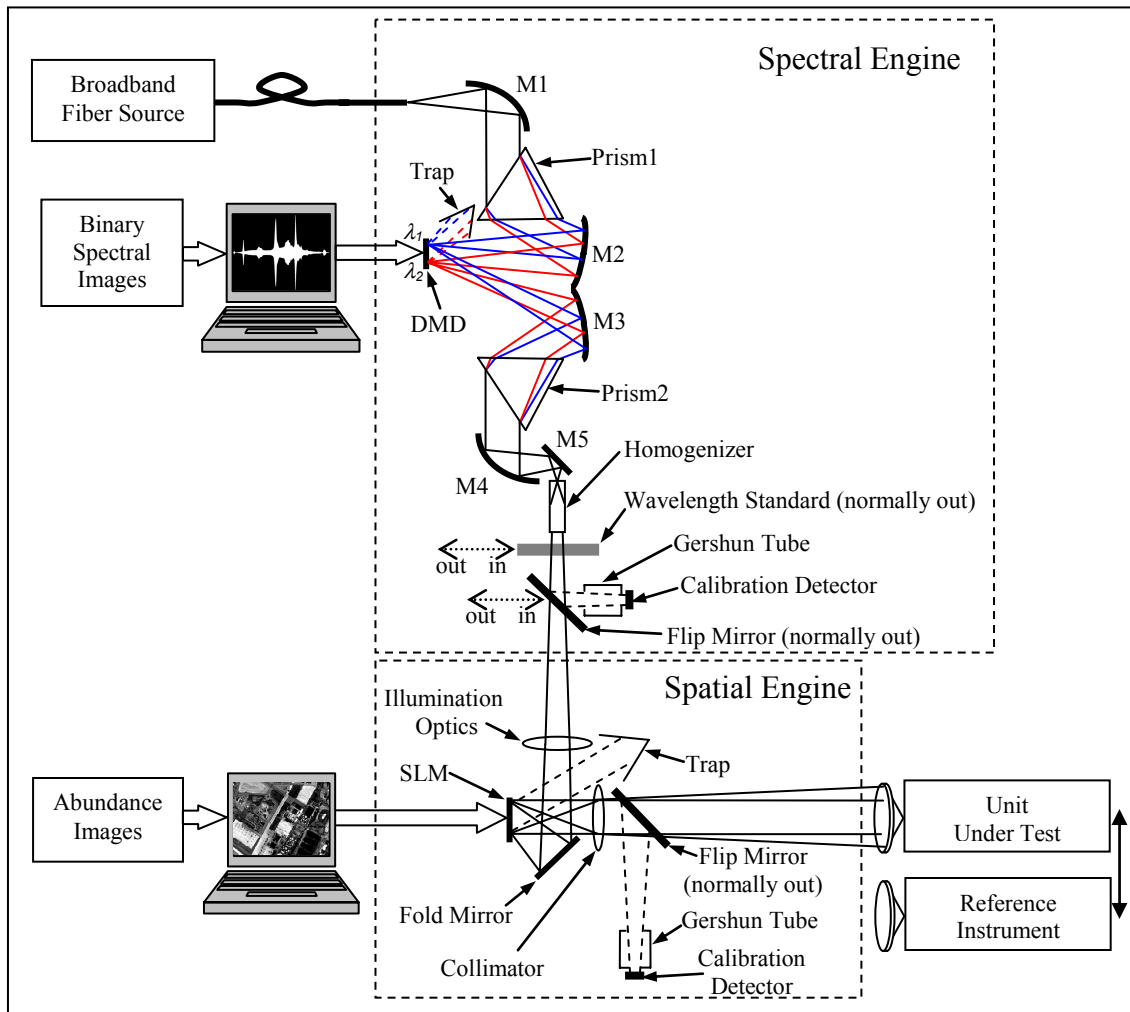


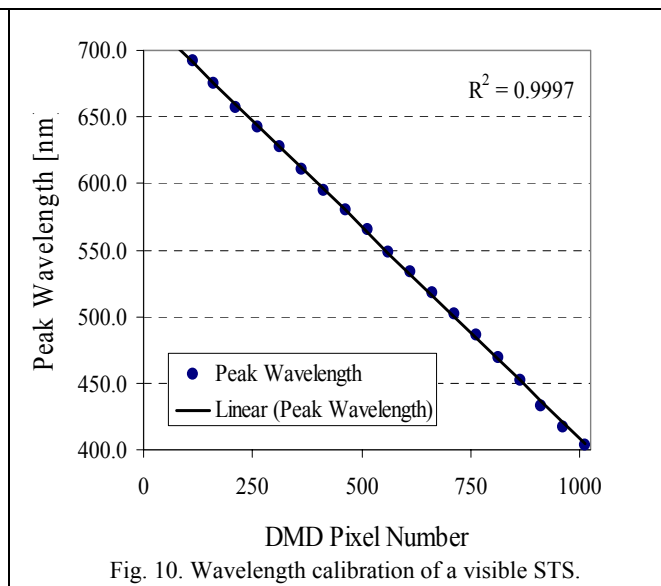
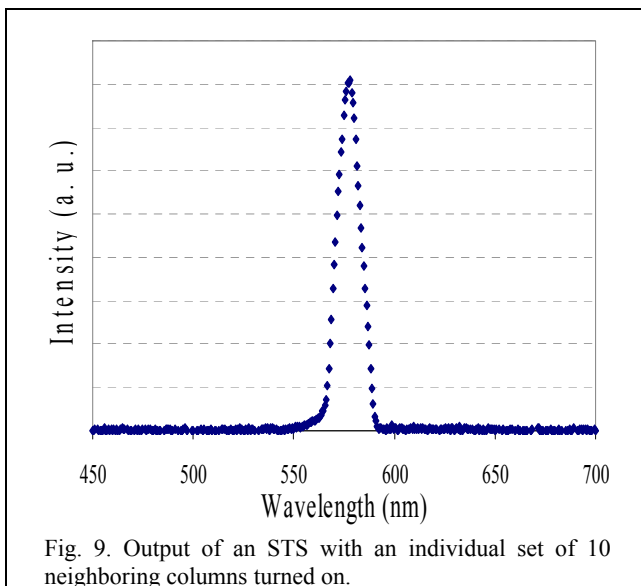
Fig. 8. Schematic of the Hyperspectral Image Projector (HIP) concept. The series of endmember spectra produced by the spectral engine illuminate the spatial engine, which synchronously projects the corresponding abundance images into the Unit Under Test (UUT). The full set of endmember spectra and corresponding abundance images are displayed within the integration time of the UUT, which then measures the projected hyperspectral scene. The Reference Instrument alternately views the same scene as the UUT and provides the absolute radiance of the scene.

## The Spectral Light Engine

The spectral engine works as follows. Light from a broadband source is fiber-coupled into the spectral engine through an entrance slit (not shown in the figure). The light is collimated by mirror M1 and reflected onto Prism1. The spectrally dispersed output of Prism1 is imaged by mirror M2 onto a DMD. This portion of the spectral engine is identical in concept and design to a conventional spectrograph, with the DMD replacing a standard two-dimensional charge-coupled device (CCD) detector array. As in a spectrograph, an image of the entrance slit is formed on the DMD array, with a particular incident wavelength imaged onto a specific columnar region. Thus, each of the DMD columns in the spectral light engine in Fig. 8 reflects a different center wavelength with a spectral bandwidth  $\lambda_1$  to  $\lambda_2$  determined by the dispersion of the prism and the width of the entrance slit.

A binary spectral image sent to the DMD from the computer determines which DMD micromirrors are "on" and which are "off." Mirrors in the 'on' state reflect the light towards mirror M3 while mirrors in the 'off' state reflect the light into a beam trap. Mirror M3 collects the light from the on-state DMD micromirrors and collimates it onto Prism 2. This prism is oriented such that spectrally dispersed light is re-combined spatially, as in a double subtractive spectrograph. Mirrors M4 and M5 focus the output of the spectral engine to a circular spot having a diameter of about 5 mm and feed it into a beam homogenizer. This is a long rectangular tube with open ends having walls made from four flat specular mirrors. Through multiple internal reflections from these highly reflective walls, the circular, spatially non-uniform input beam is reshaped into a spatially uniform output beam having a rectangular cross section that matches that of the spatial light modulator (SLM) of the spatial engine. During normal projection operations, the output beam of the homogenizer is sent directly into the spatial engine.

By turning individual columns or sets of columns on, one at a time, spectral distributions such as those shown in Fig. 9 are obtained. By turning a number of different columns on and measuring the wavelength of the collected radiation, a wavelength calibration can be obtained. The wavelength calibration of a spectral engine, shown in Fig. 10, relates the column number on the DMD array to the peak wavelength of the reflected radiation. Use of this information, along with the intensity distribution of the source (both within a column and from column-to-column), allows algorithms to be developed to generate a spectral match to a given distribution. Varying the number of mirrors turned on from 0 to 768 in a particular column gives us the dynamic range for each wavelength (assuming nearly uniform illumination of the DMD). High fidelity spectral matches to a specific target distribution can be readily achieved, with the resolution defined by the design and imaging properties of the spectrograph. The spectral engine can cycle through spectra at rates up to 16 kHz, which is the binary image update rate of the DMD.



The wavelength standard and calibration detector shown in the spectral engine of Fig. 8 are used during calibration operations. These are automated operations that typically take on the order of 30 s or less. If a calibrated, stable detector is used, the source can be calibrated absolutely against the reference detector. Si detectors covering the 350 nm to 1100 nm spectral window have been shown to be stable over years. Thus the calibration can in principle be maintained in the field for lengthy periods.

In its most basic design, the spectral engine can accept any fiber-optically coupled input source, and the output can be sent to a fiber bundle or light guide. The entrance slit width is one of the determining elements in a light engine's spectral resolution, with narrower slit widths corresponding to higher spectral resolution. With typical extended area sources, reducing the entrance slit width concurrently reduces the amount of incident flux incident on the DMD. With newly developed supercontinuum (SC) sources,<sup>10</sup> the light is generated in a single mode, photonic crystal fiber with a core diameter of approximately 5  $\mu\text{m}$ . Inputting the light from the single mode fiber directly into the spectral engine would correspond to the spectral engine having a 5  $\mu\text{m}$  wide entrance slit. Consequently, for the SC, in principle, none of the incident flux is lost as the slit is narrowed down to 5  $\mu\text{m}$ , meaning the SC-based light engine can have both high radiant flux (on the order of several mW/nm radiant flux density) and high spectral resolution.

### The Spatial Light Engine

The spatial engine works as follows. The light from the spectral engine is passed through the spatial engine illumination optics, which serves to provide spatially uniform illumination of the spatial light modulator (SLM) (Fig. 8). The SLM can be a DMD, a liquid crystal on silicon (LCOS) array, or any other suitable transmissive or reflective high-resolution spatial light modulator that can display the grey scale abundance image. We are currently using DMDs as the spatial engine SLM, but LCOS arrays could replace the DMDs. The 2D spatial image displayed on the SLM is at the focus of a collimator that fills the entrance pupil of the UUT and, alternately, the reference instrument. Unwanted spatial light from the SLM is captured by the spatial engine trap. Contrast ratio is an important consideration in the spatial projection system. Spatially scattered light, originating for example from the edges of the mirrors in the DMD, in a scene reduces the bright-to-dark contrast and can potentially limit the capability of these systems to characterize the response of satellite sensors to complex scenes. Contrast ratios of 7500:1, currently available in commercial DMD projection systems, should be sufficient for testing purposes.<sup>11</sup>

The flip mirror, Gershun tube, and calibration detector are used only for calibration. The calibration detector could in principle be a large area single element detector, or a 2-d array detector (e.g. a CCD). The calibration detector is calibrated by the reference instrument at some point, and is then expected to maintain the scale for some period of time, to be determined empirically.

The full 2D HIP works as follows. The spectral engine DMD and the spatial engine SLM both display their respective images in sync with a trigger pulse. Successive pulses trigger the production of the successive endmember spectra on the spectral engine and the corresponding abundance images on the spatial engine. The trigger is derived from the UUT so as to synchronize frame rates to avoid temporal aliasing. The complete set of endmember spectra and associated abundance images are displayed within the integration time of the UUT. Alternately, each member of the set is synchronously captured as a separate UUT frame and the frames are co-added in software.

Consider, as a simple example, a multi-spectral or hyperspectral UUT based upon a 2D staring focal plane array, with 1:1 mapping of HIP spatial pixels to UUT pixels, and consider the ideal situation in which aberrations, scattered light, air transmittance, and other contaminating effects are ignored. During its integration time, each pixel of this UUT is exposed to all endmember spectra in proportion to the corresponding levels coded for that pixel in the abundance images. Any pixel's temporally-integrated spectrum is then a linear combination of the endmember spectra. The counts from any spatial pixel of the UUT collected during the integration time then represent the radiance from the real scene from which the endmember spectra and abundance images were derived. While there are, in reality, several contaminating effects to be properly dealt with, to first order the HIP is indeed capable of simulating reality in that every pixel of a projected 2D image can have any spectrum. In addition, many of these effects, present in a real image, are properly accounted for with the reference instrument if they are stable.

Fig. 8 is merely a schematic representation of the concept. Any of the optics in Fig. 8 may of course be lenses instead of mirrors, and the dispersing elements may be transmissive or reflective gratings instead of prisms. The illumination and collimation optics in the spatial engine will be specially designed reflective or refractive subsystems, rather than single element lenses as drawn in the schematic. Multi-chip (up to 6 DMD elements) cinematic projection systems are commercially available. Utilization of multi-chip strategies improves the available power available for a given set of basis spectra because time-division multiplexing is used to produce the hyperspectral image.

### **3. THE REFERENCE HYPERSPECTRAL IMAGER**

Validation of system-level performance of the UUT does not require a perfect match between the projected scene and the input hyperspectral data cube. To validate the system-level performance of sensors, the projected scenes need to only approximate realistic scenes that the UUT will measure; however, the projected scenes must have a known spectral/spatial radiance distribution, with established uncertainties. It is the reference instrument that provides us with knowledge of the scene radiance. The current reference instrument consists of a commercially-available liquid crystal tunable filter (LCTF) in front of a CCD camera. There are two separate LCTF's with the reference instrument, covering different spectral ranges. The first LCTF operates in the visible region, from 400 nm to 720 nm with a bandwidth of 7 nm; the second LCTF operates in the NIR spectral region, from 700 nm to 1000 nm, with a bandwidth of approximately 10 nm. Data acquisition software automatically tunes the LCTF to each successive band center wavelength within a contiguous set of band center wavelengths, and the camera captures and stores the image at each wavelength. Thus the reference instrument acts as a staring-mode hyperspectral imager. Tuning times are in the millisecond range. The CCD integration time is variable, depending on the desired signal-to-noise level and the frame rate at which we operate the HIP, which is synchronized to the camera exposure signal. Capturing a full hypercube of, for instance, 42 bands typically takes tens of seconds with such a system. Consequently, the LCTF-imager may not be appropriate for acquiring dynamic scenes in real time. However, it can be a good reference instrument for use with the HIP, given that we can control the scene and ensure that it does not change during acquisition of a full data cube.

### **4. REALIZATION OF BENCH-TOP HIP**

A bench-top HIP has been realized, using both a Xe lamp as well as a supercontinuum source. Power densities of 1 mW/nm at 1 nm spectral resolution, at spatial resolutions such as 1024 x 768 and better, are feasible. Fig. 11 are digital photographs of a proof-of-principle, bench-top HIP system. The left-hand picture is a top-down view of the HIP, showing both the spectral light engine, in the center of the figure, as well as the spatial light engine, in the lower left-hand corner of the figure. The two DMD's in the HIP are enclosed in aluminum shells. The spectral engine DMD is shown in the center of the figure. The right-hand picture is a side-view of the spectral light engine. Incident radiation from a Xe-lamp source coupled into a liquid light guide is focused onto a slit, shown in the center of the figure. Radiation transmitted through the slit is collimated by a cylindrical lens, dispersed by the prism, and focused onto the DMD with a lens. The dispersed light on the DMD is barely visible in the top left-hand side of the picture.

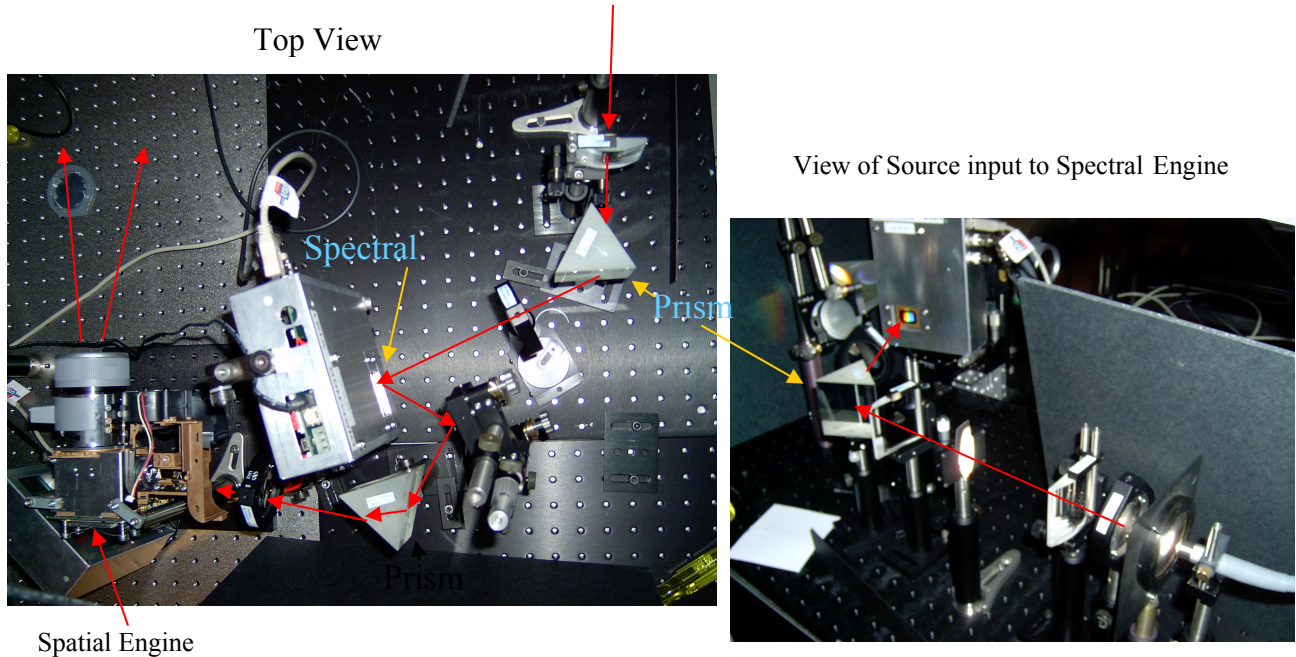


Fig. 11. Digital images of the benchtop HIP.

In Fig. 12, we show the HIP setup with a projection screen. The HIP spatial engine is shown in the bottom center of the picture. Fig. 13 is a digital image of the projected data hypercube of the gall bladder hypercube shown as an rgb image in Fig. 5 onto the screen shown in Fig. 12.

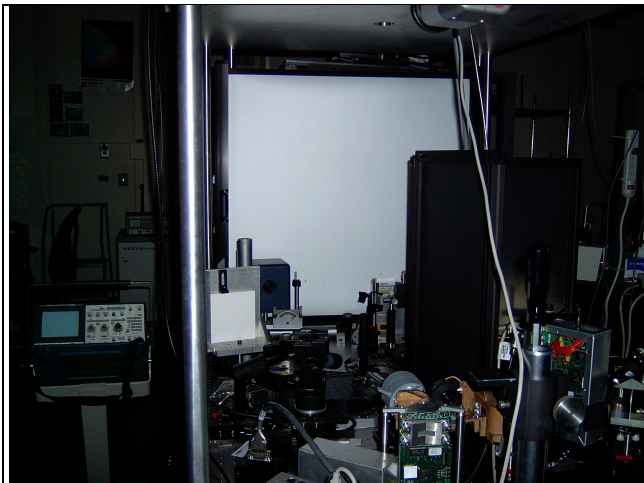


Fig. 12. The benchtop HIP setup with projector screen.



Fig. 13. A digital image of the hypercube data of the gallbladder from Fig. 5 projected on the HIP projector screen.

## 5. SUMMARY

In summary, dynamically programmable digital tissue phantoms are 2-dimensional projected images with true spectral content. Sets of projected hyperspectral scenes will be used to validate the performance of optical medical imaging systems. The projected images can be based on libraries of reference hyperspectral measurements of real tissues, or they can be simulated using modeled tissue volume scattering phase functions. The content in the projected scenes remains to

be defined by a medical standards organization, as do the metrics used in the performance validation of the instrument under test. The digital tissue phantoms defined in this work are dynamically programmable, enabling time-varying scenes to be projected. Different sets of images can be projected, depending on the intended application of the instrument under test. Consequently, the same calibration facility can be used to validate the performance of optical medical imaging systems used in a wide variety of applications. Finally, a proof-of-concept Hyperspectral Image Projector has been built and medically relevant hyperspectral data cubes have been projected with the system.

### ACKNOWLEDGEMENTS

We would like to acknowledge the guidance and support for this work by Gerald T. Fraser. This work is funded in part by the NIST Advanced Technology Program (ATP) and the NIST Office of Law Enforcement Standards (OLES).

*Note: References are made to certain commercially available products in this paper to adequately specify the experimental procedures involved. Such identification does not imply recommendation or endorsement by the National Institute of Standards and Technology, nor does it imply that these products are the best for the purpose specified. DLP and DMD are trademarks of Texas Instruments, Inc.*

### REFERENCES

- 
- [1] Pogue, B. and Patterson, M. S. "Review of tissue simulating phantoms for optical spectroscopy, imaging and dosimetry," *J. Biomed. Opt.* **11**, 041102 (2006).
  - [2] Rice, J. P., Brown, S. W. and Neira, J. E. "Development of hyperspectral image projectors," *Proc. SPIE* **6297**, 629701 (2006).
  - [3] Rice, J. P., Brown, S. W., Neira, J. E. and Bousquet, R. "A hyperspectral image projector for hyperspectral imagers," *Proc. SPIE* **6565**, 656511 (2007).
  - [4] S.W. Brown, J.P. Rice, J.E. Neira, R. Bousquet and B.C. Johnson, "Hyperspectral image projector for advanced sensor characterization," *Proc. SPIE* **6296**, 6296-02 (2006).
  - [5] Zong, Y., Brown, S. W., Johnson, B. C., Lykke, K. R. and Ohno, Y. "Simple spectral stray light correction method for array spectroradiometers," *Applied Optics* **45**, 1111-1119 (2006).
  - [6] <http://www.dlp.com/>
  - [7] Gruninger, J., Ratkowski, A. J. and Hoke, M. L. "The sequential maximum angle convex cone (SMACC) endmember model," *Proc. SPIE* **5425**, 1-14 (2004).
  - [8] N. MacKinnon, U. Stange, P. Lane, C. MacAulay, and M. Quatrevalet, "Spectrally programmable light engine for in vitro or in vivo molecular imaging and spectroscopy," *Appl. Opt.* **44**, 2033-2040 (2005).
  - [9] Brown, S. W., Rice, J. P., Neira, J. E., Johnson, B. C. and Jackson, J. D. "Spectrally tunable sources for advanced radiometric applications," *J. Res. Natl. Inst. Stand. Technol.* **111**, 401-410 (2006).
  - [10] <http://www.fianium.com>.
  - [11] dVision 30 Series projectors, Digital Projection, Inc., Kennesaw, GA.